Contrib Mineral Petrol (1999) 134: 251–263

Alexei A. Ariskin · Galina S. Barmina

An empirical model for the calculation of spinel-melt equilibria in mafic igneous systems at atmospheric pressure: 2. Fe-Ti oxides

Received: 3 March 1998 / Accepted: 7 August 1998

Abstract In order to develop models simulating the crystallization of Fe-Ti oxides in natural lavas, we have processed published experimental data on magnetite-melt and ilmenite-melt equilibria. These data include 62 *Mt*-melt and 75 *Ilm*-melt pairs at temperatures 1040–1150 °C, oxygen fugacities from *IW* to *NNO* + 2, and bulk compositions ranging from ferrobasalts to andesites and dacites. Five major cations (Fe^{3+}, Fe^{2+}, Ti^{4+}, Mg^{2+} and Al^{3+}) were considered for the purpose of describing Fe-Ti oxide saturation as a function of melt composition, temperature and oxygen fugacity at 1 atmosphere pressure. The empirically calibrated mineral-melt expression based on multiple linear regressions is: $\ln D_i = a/T + b\log f_{O_2} + c + d_1X_{Na} + d_2X_K + d_3X_P$, where D_i represents molar distribution coefficients of the given cations between *Mt*/*Ilm* and melt; X_{Na}, X_K, and X_P are the molar fractions of Na, K, and P in the melt. The empirically calibrated *Mt*-melt and *Ilm*-melt equilibria equations allowed us to develop two models for calculating crystallization temperatures of the Fe-Ti oxides in the melts with an accuracy of 10–15 °C, and compositions with an accuracy of 0.5–2 mol%. These models have been integrated into the COMAGMAT-3.5 program, improving our ability to study numerically the effects of temperature and oxygen fugacity on the stability and phase equilibria of Fe-Ti oxides. Application of this approach to the tholeiitic series of Chazhma Sill from Eastern Kamchatka (Russia) indicates oxygen fugacity conditions near *NNO* + 0.5. Numerical simulation of fractional crystallization of an iron-enriched basaltic andesite parent at these oxidizing conditions accurately reproduces the FeO-SiO_2 relations observed in the Chazhma suite.

A.A. Ariskin · G.S. Barmina
Vernadsky Institute of Geochemistry and Analytical Chemistry, Russian Academy of Sciences,
Kosygin st. 19, Moscow, 117975, Russia
Fax: (095) 938-2054, e-mail: ariskin@glas.apc.org

Editorial responsibility: T.L. Grove

Introduction

Even after decades of investigation, debate surrounding the role of magnetite crystallization in the differentiation of basalt magmas continues. This problem is directly related to genetic interpretations of siliceous differentiates, which are important members of both tholeiitic and calc-alkaline series. Most workers today agree that the andesite/diorite to rhyolite/granophyre magmas originate by fractionation of more mafic parents, however there is controversy about conditions and the dominant phases controlling the origin of silica enrichment versus iron enrichment trends (Grove and Baker 1984; Grove and Kinzler 1986; Hunter and Sparks 1987; Shi 1993; Sisson and Grove 1993; Snyder et al. 1993). A key aspect of this discussion is the relative role of magnetite and silicate mineral crystallization in the formation of the observed series of magmas. The importance of magnetite is supported by experiments showing that increasing f_{O_2} expands the magnetite field in basaltic systems, causing marked SiO_2 enrichment in derivative liquids (Osborn 1959; Presnall 1966; Eggler and Osborn 1982). The elevated pressure, which changes the phase proportions of olivine, plagioclase, and pyroxene, can also generate derivative magmas showing silica enrichment trends (Grove and Baker 1984; Grove and Kinzler 1986).

Grove and Kinzler (1986) considered Fe-Ti oxides to play a minor role in the fractionation process, with the magnetite (± ilmenite) precipitation proceeding only at the latest stages of crystallization. In contrast, experimental studies on tholeiitic and transitional to mildly alkalic basalts demonstrate that, in terms of f_{O_2} and bulk composition, the Fe-Ti oxide minerals can appear at a relatively early stage of crystallization, producing silicic liquids (Thy and Lofgren 1994; Toplis and Carroll 1995, 1996). This basic discrepancy in the petrogenetic interpretation of numerous experimental data is obviously due to the complexity of the P-T-P_{H_2O}-f_{O_2}-X systems investigated. We believe that currently available high quality experimental data cover a significant range

of conditions and compositional space to allow development of improved phase equilibria models that can be used to predict the crystallization conditions of magnetite/ilmenite – bearing mineral assemblages.

Over the last 15 years, several thermodynamic and empirical models have been developed to simulate phase equilibria for terrestrial magmas crystallizing in the compositional range from basalt to dacite (Nielsen and Dungan 1983; Frenkel and Ariskin 1984; Ghiorso 1985; Ghiorso and Carmichael 1985; Ariskin et al. 1987, 1993; Nielsen 1990; Weaver and Langmuir 1990; Longhi 1991; Camur and Kilinc 1995; Ghiorso and Sack 1995; Yang et al. 1996). However, despite the great efforts in the modernization of thermodynamic or empirical constraints, calibration techniques, and computational methods, these models still often yield poor results in the prediction of the calculated lines of descent, especially at elevated pressures and in the field of Fe-Ti oxide crystallization (Yang et al. 1996).

For example, recently Toplis and Carroll (1996) applied the MELTS program (Ghiorso and Sack 1995) to the simulation of 1 atm equilibrium crystallization of a composition, used previously in experimental studies of ferro-basaltic systems at low to high f_{O_2} (*SC1* – Toplis and Carroll 1995). Results from MELTS indicate a significant discrepancy in the observed and calculated stabilities of Fe-Ti oxides. In effect, magnetite (*Mt*) was calculated to be more stable at lower f_{O_2} (see Fig. 1 of Toplis and Carroll 1996), in contrast to experimental data, petrologic observations and common sense (Hill and Roeder 1974; Snyder et al. 1993; Nielsen et al. 1994; Toplis and Carroll 1995). A similar problem has been encountered by petrologists using the COMAGMAT program (Ariskin et al. 1987, 1993) for the modeling of crystallization paths of tholeiitic melts (Barmina et al. 1988, 1989, 1992; Frenkel et al. 1989; Chalokwu et al. 1993; Yang et al. 1996). These calculations correctly predicted the measured stability of magnetite with increasing f_{O_2}, but the calculated temperatures for *Mt* were often over-estimated by 30–40 °C relative to experimental data or petrological observations.

The purpose of this paper is to present a new model for magnetite- and ilmenite-melt equilibria, and its integration into a new version of COMAGMAT (version-3.5)[1]. This model should serve as a useful tool for igneous petrologists investigating the effects of oxygen fugacity and composition on the equilibrium temperatures, phase proportions and liquid lines of descent relevent to the crystallization of Fe-Ti oxides prior to, or simultaneously with, silicate minerals.

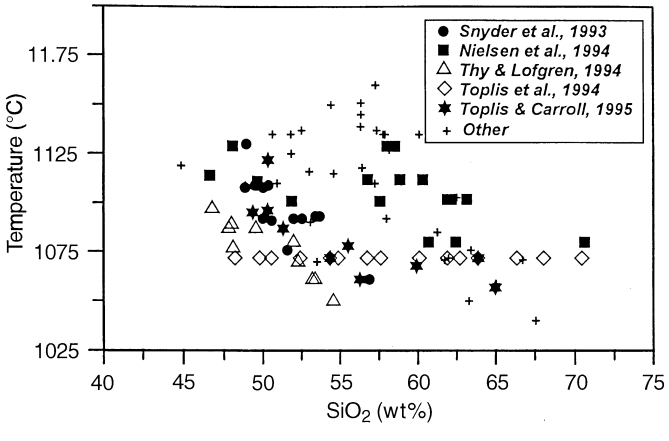

Fig. 1 Temperature – composition relations for 99 experimental glasses equilibrated with titanomagnetite plus silicate minerals at 1 atm and "dry" conditions. Extracted from the INFOREX-4.0 database (Ariskin et al. 1997) based on the following criteria: run duration >48 h, total alkalinity <7 wt%

Magnetite-melt equilibria data

Search through the INFOREX database

In order to compile an internally consistent, comprehensive database on magnetite-melt equilibria, we searched the INFOREX-4.0 experimental database (Meshalkin and Ariskin 1996; Ariskin et al. 1996, 1997) for appropriate published mineral-melt equilibria experimental data. At present, INFOREX contains melting-experiment references that access information on 254 experimental studies carried out from 1962 to 1997, including 9,113 individual runs and more than 12,600 coexisting phase compositions for 36 minerals plus glass. These data represent 3,202 1 atm experiments and 5,911 high pressure runs; 3,684 include volatile components, such as H_2O (2,154 runs are water saturated) and CO_2. Searching the database for 1 atm experiments containing glass compositions at saturation with magnetite yielded 213 experimental glass compositions, with approximately half of them representing runs with alkaline basalts and nephelinites. For further consideration, only 99 glasses from 13 experimental studies were used, which meet the two additional criteria of run duration >48 h and total alkalinity ($Na_2O + K_2O$) <7 wt%.

Sixty-six of the final group of glasses represent five of the most detailed experimental studies (Snyder et al. 1993; Nielsen et al. 1994; Thy and Lofgren 1994; Toplis et al. 1994; Toplis and Carroll 1995; and see review by Ariskin 1998). Most of them contained from 10 to 18 wt% FeO_{tot} and are generally classified as ferroba-

[1] The COMAGMAT software consists of a series of linked DOS-programs developed to simulate a variety of igneous processes including both simple crystallization of volcanic suites and the in situ differentiation of tabular intrusions (Ariskin et al. 1993). COMAGMAT is designed for melts, ranging from basaltic to dacitic compositions. The modeled elements include Si, Ti, Al, Fe_{tot} (divided into Fe^{3+} and Fe^{2+}), Mg, Ca, Na, K, P, as well as 20 trace elements. The modeled minerals include olivine (*Fo-Fa* solution), plagioclase (*An-Ab* solution plus K), three pyroxenes (augite, pigeonite, and orthopyroxene: *En-Fs-Wo* solutions plus Al and Ti), ilmenite and magnetite (Fe^{2+}-Fe^{3+}-Ti-Al-Mg solutions). The program can be used at low to moderate pressures, approximately up to 12 kb, and allows calculations to open (12 oxygen buffers) and closed system differentiation with respect to oxygen (Ariskin et al. 1987, 1993)

saltic to ferroandesitic systems (Fig. 1); TiO_2 content varied in the range of 1–5 wt%. All experimental runs were carried out using the "Pt wire loop" technique with controlled oxygen fugacities $10^{-13} < f_{O_2} < 10^{-6}$, for temperatures ranging from 1040 to 1160 °C (Fig. 2). Experimental phase assemblages produced in the experiments usually included four or five minerals plus glass, with *Mt* almost always being the fourth or fifth crystallizing phase. Plagioclase (*Pl*) is present in all experiments, whereas olivine (*Ol*), augite (*Aug*), pigeonite (*Pig*), and orthopyroxene (*Opx*) may be observed in different combinations. Forty-nine runs at log $f_{O_2} < -10$ are saturated with ilmenite (*Ilm*).

Problem of Fe^{3+}/Fe^{2+} calculations

Development of models for predicting Fe-Ti oxide stabilities is hampered by the need to estimate the relative abundances of Fe^{3+} and Fe^{2+} species in the experimental glasses, for which only total iron is usually known from microprobe analyses. At least six empirical equations have been proposed for such calculations (Sack et al. 1980; Kilinc et al. 1983; Kress and Carmichael 1988, 1991; Borisov and Shapkin 1990; Mysen 1991). Results of recent independent testing of all of the dependencies demonstrated that average deviations of the calculated Fe^{3+}/Fe^{2+} ratios from those obtained in experiments are of about 0.03–0.05, with the Borisov and Shapkin's equation producing the best fit with experimental data (Nikolaev et al. 1996). For the purpose of a preliminary investigation, this is sufficiently precise to provide adequate estimates of the Fe_2O_3 content in silicate melts to be used in the calibration of *Mt*-melt equilibria models (Ghiorso and Sack 1995). However, there are some reasons which make us doubt that such models would be realistic.

(i) If we analyze the experimental information on Fe^{3+}/Fe^{2+} equilibria available in the INFOREX database (in total, 372 experiments), one can see that the proposed Fe^{3+}/Fe^{2+} equations were calibrated on a dataset in which as much as 40% of the experiments are at $f_{O_2} > 10^{-3}$ bar, whereas only six glasses were produced at $f_{O_2} < 10^{-9}$ bar (Fudali 1965; Shibata 1967; Sack et al. 1980; Thornber et al. 1980; Kilinc et al. 1983; Kress and Carmichael 1988, 1991). The data thus over-represent highly oxidized conditions, which are outside of the main range of f_{O_2} where many of the *Mt*-melt equilibria experiments were carried out (Fig. 2). Another consequence is that these data represent the low f_{O_2} range where errors in the calculations of Fe^{3+}/Fe^{2+} ratios can reach 50 rel% (Nikolaev et al. 1996).

(ii) Time series kinetic experiments carried out at 1200 °C and $f_{O_2} = 10^{-8}$ bar indicate that 5–24 h is necessary to equilibrate FeO contents and Fe^{3+}/Fe^{2+} ratios in a homogeneous basaltic melt (Fudali 1965; Thornber et al. 1980). At $f_{O_2} = 10^{-6}$ bar this time is increased up to 48 h (Fudali 1965). Time-temperature relations (Fig. 3) between experimental data on which Fe^{3+}/Fe^{2+} equations were calibrated (n = 289) and magnetite-melt equilibria data selected (n = 99) illustrate that few Fe^{3+}/Fe^{2+} experiments had run duration >48 h, and none were at temperatures (1040–1160 °C) where magnetites were crystallized experimentally. This suggests that extrapolations of the proposed Fe^{3+}/Fe^{2+} models to the liquids saturated with Fe-Ti oxides might result in larger errors.

(iii) Data from Mössbauer spectroscopy of iron-bearing silicate liquids indicate Fe^{3+} is present in two species at $Fe^{3+}/\Sigma Fe < 0.5$, where both tetrahedrally- and octahedrally-coordinated ferric iron may coexist (Mysen et al. 1985). This means that any attempts to calculate magnetite or ferric iron activity in silicate melts from the bulk Fe^{3+}/Fe^{2+} ratios (assuming those were estimated

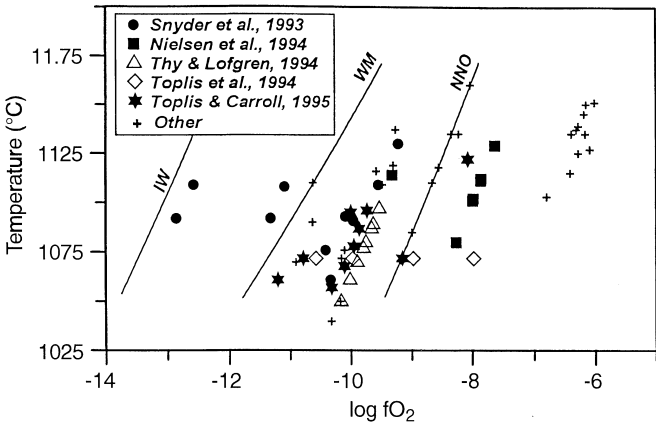

Fig. 2 Temperature – log f_{O_2} relations for 99 experimental glasses equilibrated with titanium magnetite plus silicate minerals at 1 atm and "dry" conditions. Extracted from the INFOREX-4.0 database based on the following criteria: run duration >48 h, total alkalinity <7 wt%

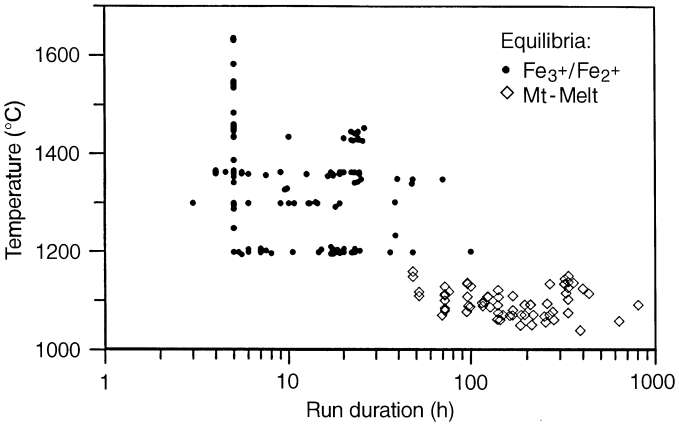

Fig. 3 Temperature – run duration relations for Fe^{3+}/Fe^{2+} and magnetite-melt equilibria studies. Two hundred and eighty-nine glasses relevant to Fe^{3+}/Fe^{2+} equilibria experiments were used to calibrate empirical equations for the calculations of Fe^{3+}/Fe^{2+} ratios in the melt (Sack et al. 1980; Kilinc et al. 1983; Kress and Carmichael 1988, 1991; Borisov and Shapkin 1990; Mysen 1991). The 99 magnetite-melt equilibria points are the same as shown in Figs. 1 and 2

correctly), would be erroneous if we do not account for the presence of Fe^{3+} ions in both tetrahedral and octahedral coordination. The absence of this information does not allow one to derive an adequate thermodynamic model for magnetite-melt equilibria, even using a solid solution model for magnetite spinels that is accurate (Sack and Ghiorso 1991; Ghiorso and Sack 1995).

Magnetite liquidus equation

Despite problems inherent in the development of thermodynamic models of magnetite-melt equilibria, an empirical approach may be useful for analysis of the effect of oxygen fugacity and melt composition on the crystallization temperature and composition of magnetite. Based on the previously selected dataset of 99 experimental glasses equilibrated with magnetite at a given oxygen fugacity and temperature, an empirical equation has been proposed, linking the liquidus temperature of magnetite with f_{O_2} and the melt composition parameters of Ariskin (1998):

$$10^4/T = (b_0 + b_1 X_{SiO_2} + b_2 X_{TiO_2} + b_3 X_{FeO_{tot}}) \log f_{O_2} + c + d_1 X_{SiO_2} + d_2 X_{TiO_2} + d_3 X_{FeO_{tot}} + d_4 X_{P_2O_5} \quad (1)$$

where X_i is the molar fraction of a melt component calculated on a single cation basis (SiO_2, $AlO_{1.5}$, $NaO_{0.5}$, $PO_{2.5}$, etc.), whereas b_i, c, and d_i are the regression coefficients (see Table 1). The four compositional parameters in Eq. 1 (SiO_2, FeO_{tot}, TiO_2 and P_2O_5), were selected from the results of 30 least square calculations with varying number and type of melt components. Note that the compositional terms related to log f_{O_2} permit one to account for the variability of the effect of oxygen fugacity in different compositional systems, as was proposed by Borisov and Shapkin (1990).

Using the regression parameters from Table 1, Eq. 1 allowed us to calculate the magnetite liquidus temperatures for experimental melts used to calibrate the expression. One can see from this internal check (Fig. 4) that despite a few large deviations $\Delta = T_{exp} - T_{calc}$ of 40–50 °C, 90% of the calculated temperatures fall within 15 °C of the experimental temperatures, with the average deviation being ±9.3 °C.

Table 1 Regression coefficients for Eq. 1

Parameter	Coefficient	Std deviation (1σ)
b_0	−0.6232	0.0205
b_1	0.6826	0.0359
b_2	4.0438	0.9327
b_3	0.8251	0.2567
c	0.0159	0.0686
d_1	8.3626	0.2804
d_2	35.9674	8.0819
d_3	10.7347	2.1842
d_4	12.4418	2.3521

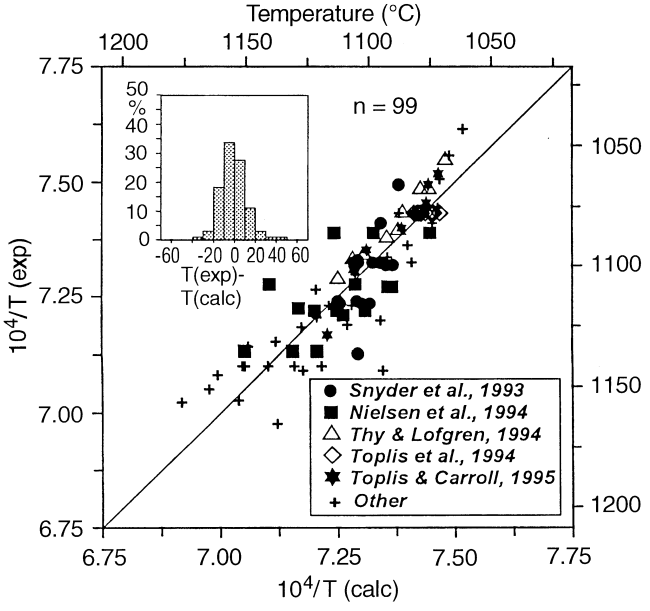

Fig. 4 Experimental vs calculated temperatures for 99 magnetite saturated liquids in ferrobasaltic to andesitic systems. Calculations of the magnetite temperatures were conducted using Eq. 1 and the regression parameters from Table 1. The histograms show differences (in rel% of total number of runs) between measured and calculated temperatures

Results of applications of Eq. 1 to melt compositions similar to natural basaltic systems demonstrate that the calculated *Mt* crystallization temperatures have a complex dependence on oxygen fugacity (Ariskin 1998). For ferrobasaltic and ferroandesitic melts with moderate contents of FeO (< 15–16 wt%) and TiO_2 (< 2 wt%), the magnetite liquidus has a fairly steep slope of about 20 °C/log f_{O_2}, whereas for Fe-Ti basalts with 4–5 wt% TiO_2 and 17–18 wt% FeO (Brooks et al. 1991) the *Mt* liquidus temperatures are virtually independent of oxygen fugacity, varying in the vicinity of 1100 °C within ±5 °C. Another important observation concerns a high sensitivity of the *Mt* crystallization temperatures to P_2O_5. Calculations using Eq. 1 indicate that addition of 1 mol% of P_2O_5 to a basaltic melt will decrease the *Mt* crystallization temperature by 20 °C (Ariskin 1998). This is in good agreement with the experimental data of Toplis et al. (1994).

Magnetite-melt equilibrium equations

Although the empirical Eq. 1 is useful for a general analysis of the effect of f_{O_2} on magnetite crystallization temperatures at a fixed melt composition, there are two reasons why it should not be used for the development of empirical models describing the magnetite-melt equilibrium.

(i) It was constrained independently of experimental *Mt* compositions, which usually include Fe_2O_3, FeO, TiO_2, as well as some amounts of MgO and Al_2O_3.

(ii) It was constrained by least square fitting, which estimated the effect of melt composition to be much higher than the effect of f_{O_2}. Because of this, our attempts to integrate this equation to the COMAGMAT program (Ariskin et al. 1993) were not successful. Simulations of *Mt* crystallization resulted in depletion of melts in FeO_{tot} beyond that compatible with observation, resulting in the conclusions that changes of the *Mt* equilibrium temperature with f_{O_2} could not be accurately calculated. Below, we will consider results of an alternative calibration of an empirical magnetite-melt equilibria model which will allow us to account for the effect of magnetite composition for a wide range of oxygen fugacities.

End-member magnetite-melt geothermometers

The core of the differentiation program COMAGMAT is a set of empirically calibrated equations, called hereafter geothermometers, which describe mineral-melt equilibria in terms of pressure, temperature, and liquid compositions (Ariskin et al. 1987, 1993). Each mineral-melt model includes several end-member geothermometers to account for the mineral solid solutions. Our purpose here is to calibrate a set of magnetite-melt equilibria equations, accounting for five main *Mt* cations, such as Fe^{3+}, Fe^{2+}, Ti^{4+}, Al^{3+}, and Mg^{2+}. As an initial step we tried to apply an empirical approach similar to that used to develop the SPINMELT program, describing chromian spinel-melt equilibria (Ariskin and Nikolaev 1996). However, this attempt was not successful, mostly due to difficulties related to the calculation of the activities of ferric species in the melt (see discussion above). In this paper, we used a simplified technique, including multiple regressions in the form:

$$\ln D_i = a/T + b \log f_{O_2} + c + d_1 X_{Na} + d_2 X_K + d_3 X_P \quad (2)$$

where D_i represents the molar distribution coefficients of Fe^{3+}, Fe^{2+}, Ti^{4+}, Al^{3+}, and Mg^{2+} between Fe-Ti spinel and melt; X_{Na}, X_K, and X_P are the molar fractions of Na, K, and P in the melt calculated on a single cation basis; a, b, c, d_1, d_2, and d_3 are the regression coefficients. Note, that the value of D_i for Fe^{3+} and Fe^{2+} is calculated as X_i^{Mt}/X_{Fe}^{L}, where Fe is total iron in the melt without separating into ferric and ferrous species. To perform this linear best fit calculation, we had to use a subset of the data utilized for the calibration of the *Mt* liquidus expressions (Fig. 1, Table 1), because only 74 of the 99 experiments with cited equilibrium magnetite provided mineral compositions. When the data set was further constrained by Cr_2O_3 content (*Mt*) < 3 wt%, $46 < SiO_2$ (melt) < 70 wt%, and P_2O_5 (melt) < 1.5 wt%, the dataset was reduced to 62 magnetite/melt pairs.

Calibration of the second linear model was performed in two stages. First, the regression parameters were calculated for the entire set of 62 coexisting magnetite-melt pairs. Using the regression parameters, experimental phase compositions, and f_{O_2} values, magnetite-melt equilibrium temperatures were calculated. A calculated temperature more than three times the average standard deviation of the experimental values was considered evidence that an experiment did not achieve equilibrium; such experiments were excluded from the second stage processing of the data. Typically, 10–12 points with temperature deviations from 60 °C to 150 °C were excluded for each set of calculations. Multiple linear regression parameters for five magnetite-melt equilibria equations which best fit the dataset are given in Table 2. The calculated regression parameters indicate strong temperature, f_{O_2} and melt composition controls on the distribution coefficients.

Using the geothermometers given in Table 2, one can invert the calculations to obtain *Mt*-melt equilibria temperatures for the calibration database liquid compositions. Comparison of the calculated and experimental temperatures for the five end-member geothermometers indicate an average accuracy of approximately 10 °C (Fig. 5). The inverse calculations for equilibrium constants lead us to expect that the final magnetite-melt equilibrium model based on the equations will also accurately reproduce *Mt* compositions (next section).

Table 2 Regression constants for magnetite-melt and ilmenite-melt geothermometers calibrated in "dry" systems at 1 atm[a]

Component	a	b	c	d_1	d_2	d_3
Magnetite						
Fe^{3+} (n = 50)	20964.7 (*2075.6*)	0.6159 (*0.0252*)	−8.8187 (*1.4730*)	−10.1838 (*2.8384*)	32.7525 (*2.9031*)	−14.2506 (*4.3306*)
Fe^{2+} (n = 53)	17013.8 (*1815.3*)	0.1042 (*0.0189*)	−10.1728 (*1.2499*)	−1.5938 (*2.6404*)	14.1291 (*2.4465*)	−11.7925 (*3.5610*)
Al (n = 51)	−17128.7 (*2079.7*)	0.0105 (*0.0202*)	11.5136 (*1.4272*)	−0.8377 (*2.7046*)	−4.8338 (*2.4627*)	5.8200 (*3.6922*)
Mg (n = 52)	14971.4 (*2370.5*)	0.2021 (*0.0255*)	−8.2121 (*1.6317*)	−10.2151 (*3.3928*)	13.6451 (*2.8096*)	−25.1426 (*4.6924*)
Ti (n = 43)	27422.6 (*2325.7*)	−0.1336 (*0.0232*)	−20.3655 (*1.5963*)	10.5126 (*3.2761*)	22.0278 (*3.2829*)	−10.3297 (*4.0910*)
Ilmenite						
Fe^{3+} (n = 65)	18933.4 (*5796.2*)	0.8475 (*0.0469*)	−8.6100 (*4.3982*)	35.4214 (*9.8997*)	28.9571 (*9.6089*)	−8.6859 (*7.4175*)
Fe^{2+} (n = 56)	2649.1 (*903.4*)	0.0544 (*0.0084*)	−0.4271 (*0.6935*)	−1.8146 (*1.7981*)	20.6115 (*2.4139*)	−1.7339 (*1.3306*)
Al (n = 66)	−14947.7 (*2436.5*)	0.1778 (*0.0204*)	9.4357 (*1.8763*)	0.1175 (*4.4802*)	3.4801 (*4.6040*)	2.6951 (*3.4255*)
Mg (n = 53)	904.8 (*1044.4*)	0.0340 (*0.0087*)	0.1111 (*0.7864*)	−1.6455 (*1.7008*)	14.3103 (*1.6868*)	−6.8648 (*1.3100*)
Ti (n = 72)	12245.2 (*974.7*)	0.0178 (*0.0080*)	−6.6774 (*0.7474*)	5.8720 (*1.8045*)	25.2774 (*1.7771*)	−5.3331 (*1.4075*)

[a] The regression constants correspond to mineral-melt distribution coefficients D_i calculated as per linear model (Eq. 2): standard deviations (1σ) for each constant in parentheses.

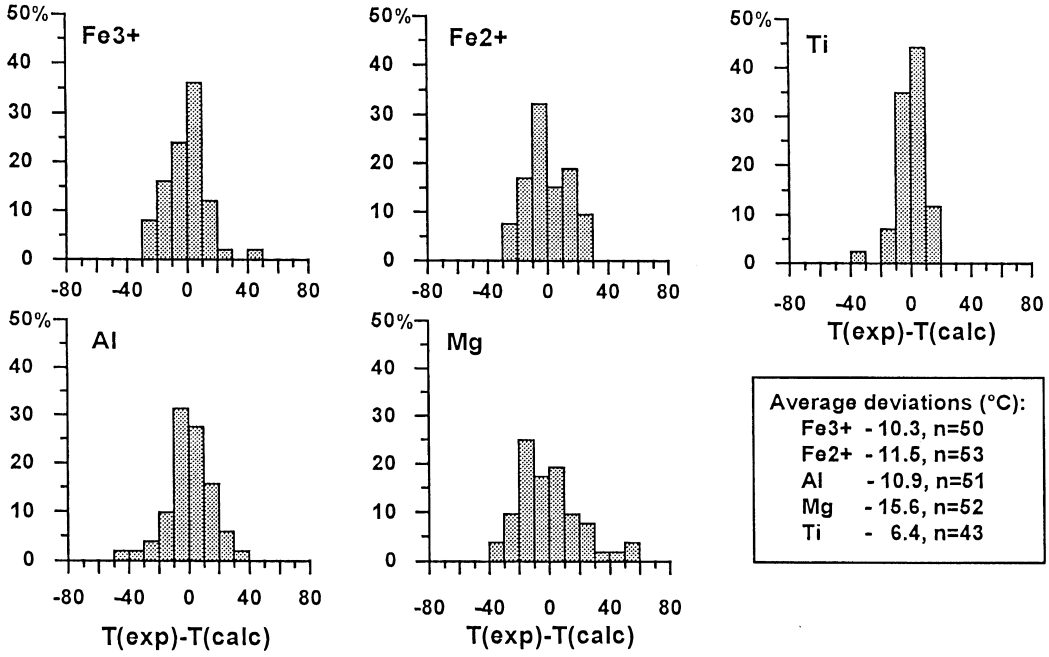

Fig. 5 Histograms of the differences between measured and calculated temperatures for experimental liquids equilibrated with magnetites of known composition. Calculations of the magnetite temperatures were conducted using geothermometers Eq. 2 and the regression parameters from Table 2 for the five cations under consideration

Model test for the magnetite-melt geothermometer

The individual end-member geothermometers can be combined into a single *Mt*-melt geothermometer, which calculates crystallization temperatures and compositions of magnetite as a function of oxygen fugacity and liquid composition (Ariskin and Nikolaev 1996). This combination includes relationships between the empirical equations for each component (Eq. 2), the regression parameters given in Table 2, and a simple magnetite stoichiometry equation, such as:

$$X^{Mt}_{Fe^{3+}} + X^{Mt}_{Fe^{2+}} + X^{Mt}_{Ti^{4+}} + X^{Mt}_{Al^{3+}} + X^{Mt}_{Mg^{2+}} = 1. \quad (3)$$

This system of equations can be solved iteratively using the algorithm described by Ariskin et al. (1993). To test this "magnetite" algorithm, we calculated crystallization temperatures and compositions of magnetites co-existing with the 32 experimental melts used to calibrate the end-member magnetite geothermometers. These 32 glasses were produced in experiments with run duration >100 h and represent those magnetite-melt compositions most likely to have achieved equilibrium (Grove and Juster 1989; Snyder et al. 1993; Toplis et al. 1994; Toplis and Carroll 1995). Results of these calculations (Fig. 6) demonstrate both the reproducibility of experimental data and the internal consistency of the end-member geothermometers as combined into a single magnetite equilibrium model.

The modeled magnetite compositions reproduce those observed in experiments with an average precision of ± 2.27 mol% for Fe^{3+}, ± 2.31% for Fe^{2+}, ± 0.48 for Al^{3+}, ± 0.40% for Mg^{2+}, and ± 1.28% for Ti^{4+}. Note that the accuracy for the bulk iron content calculations (Fe^{3+} + Fe^{2+} in magnetite) is of about 1 mol%. The calculated temperatures reproduce the experimental temperatures within 9.2 °C. In general, the magnetite model works best in the range $WM < f_{O_2} < NNO$. At higher values of f_{O_2}, the results overestimate the equilibrium temperatures of 15–30 °C. Thus, the observed internal consistency of both calculated temperatures and magnetite compositions demonstrates that a general model based on this empirical basis can adequately calculate *Mt*-melt equilibria.

New version of COMAGMAT model

This new magnetite-melt algorithm has been integrated into the COMAGMAT-3.5 model (Ariskin et al. 1993; modified 1997) which now incorporates magnetite and orthopyroxene equilibria more accurately (Bolikhovskaya et al. 1996). It allows one to simulate crystallization in systems both open and closed with respect to oxygen, including improvements concerning calculations of molar mineral-melt distribution coefficients for TiO_2 in clino- and orthopyroxenes, and K_2O in plagioclase. Another important modification includes the integration of a new ilmenite-melt equilibrium model.

Development and testing ilmenite-melt geothermometers

To simulate ilmenite crystallization in the previous COMAGMAT-3.0 model (Ariskin et al. 1987, 1993) we used a modified empirical model proposed by Nielsen

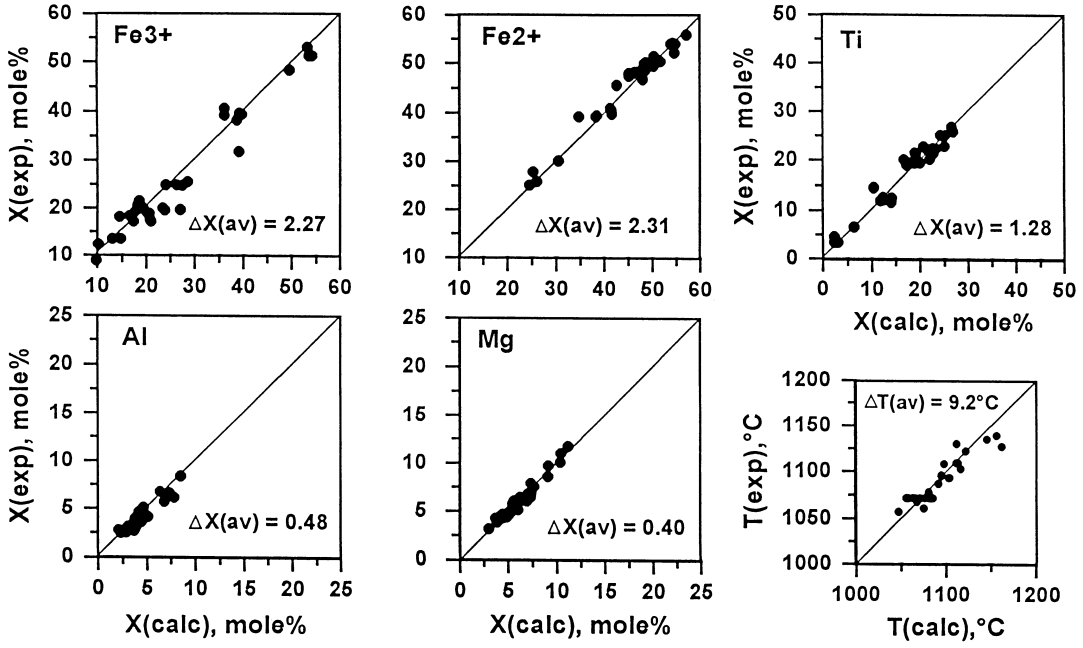

Fig. 6 Comparison of magnetite compositions and temperatures observed in experiments with those calculated at a given oxygen fugacity and liquid composition using the *Mt*-melt equilibria model. The values of $\Delta X(av)$ and $\Delta T(av)$ represent average deviations of the calculated parameters from experimental values

and Dungan (1983). It allowed us to obtain the appearance of ilmenite at low oxygen fugacities, however the calculated temperatures were systematically underestimated by 20–30 °C. It resulted in late crystallization of ilmenite below melt TiO_2 contents of 6–7 wt%. To make the ilmenite calculation more realistic, a new *Ilm*-melt model was calibrated based on the same approach as was used for magnetite.

Initially, a global search for ilmenite-melt equilibria data was conducted using the INFOREX-4.0 database with the same experimental constraints as were used during search for magnetite-melt information. The search resulted in a database including 85 coexisting ilmenite and glass compositions from five experimental studies (Juster and Grove 1989; Snyder et al. 1993; Auwera and Longhi 1994; Toplis et al. 1994; Toplis and Carroll 1995). Due to a deficit of Fe^{3+} cations, some of the experimental ilmenites could not be recast to a realistic stoichiometry; these data were excluded from the basic dataset. In addition, few experimental points, for which oxygen fugacity is unknown, were also excluded. Finally, a dataset of 75 coexisting *Ilm* and melt compositions was used for calibration of the expressions.

All the experimental runs have durations >48 h and were carried out at conditions of controlled oxygen fugacities $10^{-13} < f_{O_2} < 10^{-8}$, for temperatures ranging from 1050 to 1150 °C. Most of the experimental glasses are ferrobasaltic to ferroandesitic compositions, with total alkalinity (Na_2O + K_2O) <7 wt%. Mathematical processing of this information has been conducted in the form of least square fitting as per Eq. 2 for the cations Fe^{3+}, Fe^{2+}, Ti^{4+}, Al^{3+}, and Mg^{2+}. Similar to the fitting of *Mt*-melt equilibria data described above, a two-stage calibration process was used. The second stage entailed exclusion of all of points with large calculated temperature deviations. Multiple linear regression parameters for five ilmenite-melt equilibria equations that best fit this dataset are given in Table 2.

These parametrizations have been combined with a general *Ilm* stoichiometry equation:

$$X^{Ilm}_{Fe^{3+}} + X^{Ilm}_{Fe^{2+}} + X^{Ilm}_{Ti^{4+}} + X^{Ilm}_{Al^{3+}} + X^{Ilm}_{Mg^{2+}} = 1 \quad (4)$$

to form a system of equations that allow one to calculate ilmenite equilibrium temperatures and compositions, if given oxygen fugacity and melt composition. The 64 ilmenite-melt experiments that were deemed to have approached equilibrium were used in the determination of the internal consistency of the expressions. These experiments had run duration >100 h covering the range of oxygen fugacities $-12.6 < f_{O_2} < -9$ (Fig. 7).

These results establish the level of accuracy of the ilmenite temperature calculations (average 7.2 °C). The modeled ilmenite compositions also reproduce those of experimental products with precision of 1 mol% for Fe^{3+} and Fe^{2+}, ±0.07% for Al^{3+}, ±0.48% for Mg^{2+}, and ±0.52% for Ti^{4+}. This proposed ilmenite-melt crystallization algorithm has been integrated into the COMAGMAT-3.5 model, so that this program can now be applied to a wide range of mafic igneous systems including those saturated with Fe-Ti oxides. It is noteworthy that this model permits the user to obtain compositions of modeled magnetite and ilmenite both in the form of single cation fractions (Fe^{3+}, Fe^{2+}, Al^{3+}, Mg^{2+}, and Ti^{4+}) and in the form of X_{Ulv} and X_{Ilm} parameters calculated on the basis of the widely used equations of Stormer (1983). Below, we will consider results from the new version of COMAGMAT on an

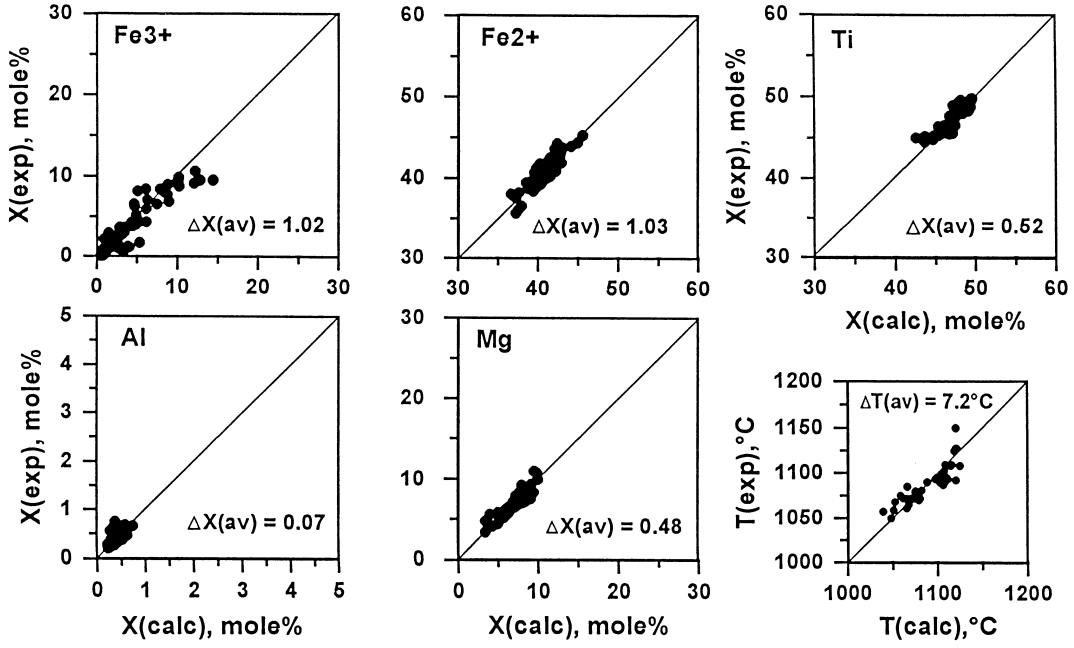

Fig. 7 Comparison of ilmenite compositions and temperatures observed in experiments with those calculated at a given oxygen fugacity and liquid composition using the *Ilm*-melt equilibria model. The values of ΔX(av) and Δ T(av) represent average deviations of the calculated parameters from experimental values

independent experimental dataset (Hill and Roeder 1974) and recent data of Toplis and Carroll (1995), which specify the field of coexistence of magnetite and ilmenite in detail.

Results from COMAGMAT crystallization model

Hill and Roeder (1974) presented experimental results on the stability of Fe-Ti and chromian spinels in terms of oxygen fugacity for a natural ferrobasalt composition (*GL-RHB*, Table 3). For almost 20 years this was the only study where the dependence of magnetite crystallization temperatures on f_{O_2} was investigated in a systematic way. These data are independent of our calibration experiments; they were carried out at 1 atm and cover a wide range of oxygen fugacities $-14 < \log f_{O_2} < -0.68$. A series of COMAGMAT-3.5 calculations simulating the course of equilibrium crystallization at 1 atm has been performed for the range $-10 < \log f_{O_2} < -6$ using the *GL-RHB* composition as the starting composition. These calculations were conducted at five fixed oxygen fugacities ($\log f_{O_2} = -6, -7, -8, -9$, and -10) with the crystallization increments of 1 mol%, up to the temperatures of 1100 °C (Fig. 8).

Table 3 Compositions of rocks and melts used in experimental studies and in the COMAGMAT calculations simulating the course of equilibrium and fractional crystallization[a]

Sample	Experimental studies		Chazhma Sill (Eastern Kamchatka)					
	Hill and Roeder (1974)	Toplis and Carroll (1995)	Plagiodolerite and its "trapped" melt		Fine-grained rocks of leucocratic layers			
	GL-RHB	*SC1*	*PD* (22)	*PD-30*	*GD1* (2)	*GD2* (4)	*DR* (3)	*GR* (3)
SiO_2	51.09	48.75	51.69	51.70	53.78	54.65	59.45	64.33
TiO_2	2.07	2.90	1.28	1.87	1.92	1.92	1.44	0.93
Al_2O_3	15.34	14.89	18.47	13.65	14.11	14.20	14.28	15.10
FeO*	13.30	13.09	10.24	14.43	13.47	12.91	10.32	7.48
MnO	–	–	0.16	0.22	0.21	0.23	0.25	0.16
MgO	6.17	6.49	4.15	5.30	3.95	3.60	2.44	1.25
CaO	8.96	10.89	10.22	9.28	8.16	7.52	5.67	3.46
Na_2O	1.99	2.70	2.52	2.09	2.66	3.03	3.33	3.79
K_2O	1.09	0.30	1.04	1.11	1.41	1.55	2.18	3.20
P_2O_5	–	–	0.24	0.35	0.33	0.38	0.64	0.30

[a] Experimental, natural and modeled compositions were normalized to 100 wt% with total Fe as FeO. *PD* average plagiodolerite (n = 22); *PD*-30 a residual melt after 30% equilibrium crystallization of *PD* including subtraction of 28.7 wt% *Pl* ($An_{61.6}$) and 1.3 wt% *Ol* ($Fo_{70.4}$); *GD1* average "primitive" ferrogabbro-diorite (used as a parental magma in the COMAGMAT simulations shown in Fig. 11); *GD2* average ferrogabbro-diorite; *DR* average ferrodiorire; *GR* average Fe-rich granophyre.

Despite run durations in these experiments of less than 90 h (most < 48 h), these results demonstrate that the new COMAGMAT model realistically reproduced the experimental crystallization sequences. Magnetite was calculated to be the first phase to crystallize at $f_{O_2} = 10^{-6}$ bar, and the fourth phase crystallizing at $f_{O_2} = 10^{-9}$ bar. Calculated magnetite crystallization temperatures differ from those observed in experiments by no more than 10–15 °C, i.e. within the accuracy of the proposed magnetite model (Fig. 6). Note, that the dependence of the calculated *Mt* liquidus on oxygen fugacity changes with f_{O_2}: 30–35 °C/log f_{O_2} at $-7 < \log f_{O_2} < -6$, and 15 °C/ log f_{O_2} at log $f_{O_2} < -10$.

Another comparison of experimental and modeled phase diagrams (Fig. 9) is calculated for the synthetic ferrobasalt *SC1* (Table 3). These calculations were used to constrain the stability of magnetite and ilmenite at different oxygen fugacities (Toplis and Carroll 1995, 1996). The phase diagram in Fig. 9B was constructed from the results 17 calculations simulating equilibrium crystallization of *SC1* composition at oxygen fugacities parallel to the *QFM* buffer, in the range from $\Delta QFM = -2.5$ to $\Delta QFM = +1.5$ with an increment of 0.25. To minimize the effect of errors in calculated olivine and plagioclase crystallization temperatures on stability of Fe-Ti oxides, those were increased by 5 °C for olivine and decreased by 15 °C for plagioclase (Ariskin et al. 1993). Comparison of the experimental and modeled diagrams indicates that COMAGMAT-3.5 accurately predicts the crystallization sequence both for silicate minerals and oxides, with the errors for magnetite and ilmenite being within 10–12 °C.

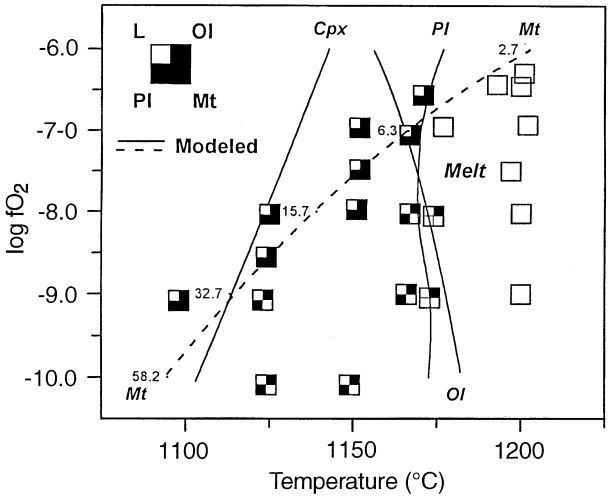

Fig. 8 Comparison of experimental and calculated phase assemblages produced during equilibrium crystallization of the *GL-RHB* ferrobasaltic melt (Table 3). Experimental data are from Hill and Roeder (1974). Calculations were carried out using the COMAGMAT-3.5 phase equilibria model described in the paper. To minimize the effect of errors in the calculated olivine and plagioclase crystallization temperatures on the stability of magnetite, those temperatures were increased by 15 °C for olivine and 10 °C for plagioclase (Ariskin et al. 1993). Digits near the *Mt* saturation line indicate X_{Ulv} in magnetite calculated from Stormer (1983)

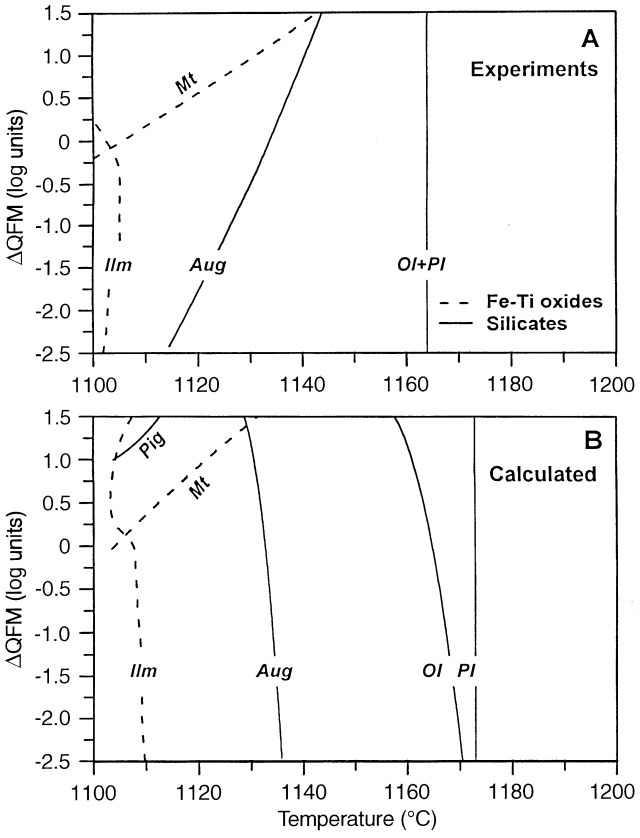

Fig. 9A, B Phase diagrams for a ferrobasaltic composition – *SC1* (Table 3). **A** Experimental data from Toplis and Carroll (1995, 1996). **B** Calculations carried out using the COMAGMAT-3.5 phase equilibria model. To minimize the effect of errors in the calculated olivine and plagioclase crystallization temperatures on the stability of Fe-Ti oxides, the olivine temperature was increased by 5 °C and plagioclase was decreased by 15 °C (Ariskin et al. 1993). *Aug* augite, *Pig* pigeonite

These data provide important information on the crystallization proportions of the Fe-Ti oxides, which are difficult to obtain experimentally. Directly below the calculated magnetite liquidus, the modeled proportions of *Mt* are high (35–40%), in agreement with independent estimates by experimentalists (Hill and Roeder 1974; Toplis and Carroll 1996). However for the main range of the crystallization of $Ol + Pl \pm Aug + Mt$ assemblage, the amount of magnetite to crystallize ranges from 16-22%. Note that *this is true only for the calculations conducted parallel to the QFM buffer.* Any changes in the buffered T-f_{O_2} trajectory will result in changes in the magnetite crystallization proportions. The calculated proportion of ilmenite is more constant, varying from 8 to 14 wt%. During simultaneous precipitation of magnetite and ilmenite, signatures of peritectic (reaction) relations between these two phases were not observed.

Modeling the formation of ferrodiorites from the Chazhma sill, Kamchatka

Geological setting, field relations and previous work

The Chazhma sill is part of the Paleocene-Eocene volcanic-plutonic association of the Kronotsky Peninsula, Eastern Kamchatka, Russia (Barmina et al. 1988). This igneous suite is approximately 4 km thick, and consists of numerous flows of pillow lavas and 20–200 m thick sills. The dominant lithology is high-Al basalts containing up to 24 wt% Al_2O_3. These plagiophyric basalts, plagioclase-rich diabases and hypabyssal plagiodolerites are spatially associated with rare ferrobasalts and ferroandesites in a tholeiitic series (Barmina et al. 1989) generated early in the formation of the Kurile-Kamchatkan Island arc.

The Chazhma sill is located in the region of Chazhma Cape at the northeast end of the Kronotsky Peninsula. The thickness of the sill varies in the range of 25–40 m. Its rocks are exposed as craggy cliffs extending along the Pacific ocean coast for $\sim$ 1.5 km, with well defined upper and lower contacts with country volcanic-sedimentary rocks. This sill is composed mostly of fresh medium-grained mesocratic plagiodolerites, which contain an average of 18 wt% Al_2O_3 (Table 3). These porphyritic rocks contain 20–30 vol% of plagioclase- and rare olivine-phenocrysts. The groundmass is composed of plagioclase, *Cpx* (augite and pigeonite), Fe-Ti oxides, and a small amount of glassy and granophyric material (Barmina et al. 1988).

A characteristic feature of the Chazhma sill is a large number of fine- to coarse-grained leucocratic layers, pipes, diapirs and micropegmatite veins, embedded between massive plagiodolerites (Fig. 10). As the proportion of plagioclase phenocrysts in these leucocratic rocks decreases, olivine disappears, whereas the fabric of clinopyroxenes and magnetite indicates these minerals are primary liquidus phases. The groundmass is enriched in glass and granophyre, with minor apatite, hornblende and biotite. The observed field relations allowed us to conclude that there was no large scale mixing between these mesocratic and leucocratic magmas. This leucocratic material was probably injected into the plagiodolerite magma body simultaneously with, or just after emplacement, as the body began to crystallize (Barmina et al. 1988).

The composition of the leucocratic rocks was found to vary from Fe-rich gabbrodiorites to Fe-rich diorites and granophyres, similar to relations observed between Kronotsky ferrobasaltic andesites, ferroandesites and ferrodacites (Table 3, Fig. 11D). Previous geochemical studies have also demonstrated that the compositions of Chazhma layers display a coherent trend of decreasing V, Cr, Ni, Sc with increasing silica content, whereas the incompatible element concentrations, such as REE, Ba, Rb, and Hf, systematically increase with SiO_2 (Barmina et al. 1992).

The presence of Ti-magnetite crystals in glomerocrysts with plagioclase ($An_{50–65}$) and Ca-rich to pigeonite pyroxenes, suggests that this Chazhma suite represents simple derivatives formed by fractional crystallization from a ferrobasalt or basaltic andesite parent. Creation of the new "magnetite" model makes it possible to attempt a quantitative genetic model of this tholeiitic series, including both estimates of redox conditions and numerical simulation of the primary chemical features of the crystallization products.

Estimate of redox conditions and modeling parental magma evolution

To estimate the oxidation conditions during crystallization of the Chazhma ferrodiorites, we propose a new

Fig. 10 Leucocratic layers and micropegmatite veins of silicic material, embedded between mesocratic massive plagiodolerites. Hammer is 80 cm long

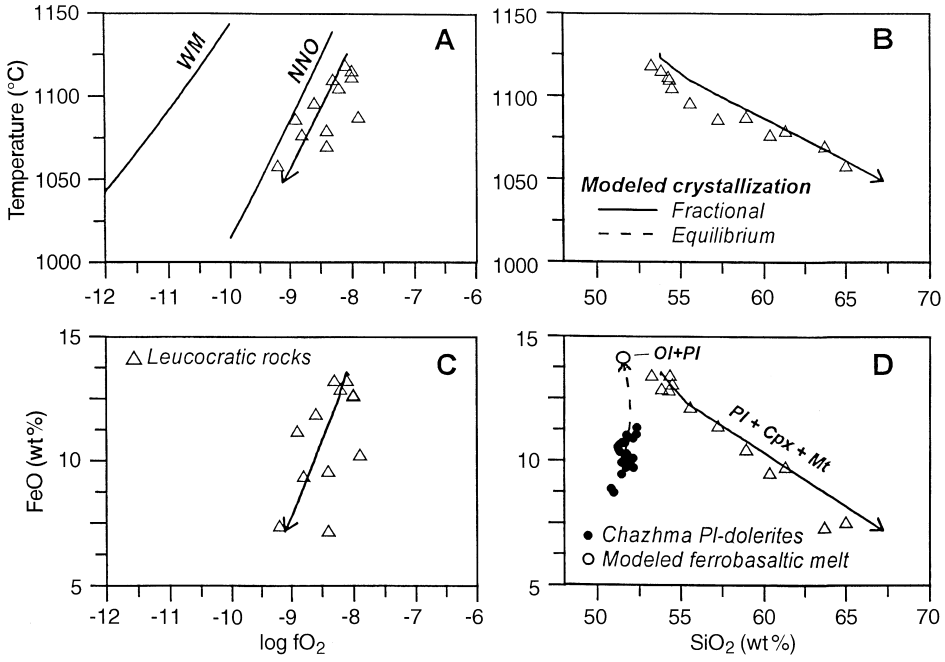

Fig. 11A–D Estimates of redox conditions and results of calculations modeling the formation of the Chazhma sill gabbro- and granodiorites. **A** Each *triangle* represents a value of log f_{O_2} and temperature at which this rock (melt) is simultaneously saturated with plagioclase and magnetite. *Pl* temperatures are calculated using geothermometers from the COMAGMAT model (Ariskin et al. 1993), whereas those for magnetite are calculated using the "magnetite" model presented in this paper. **B** *Triangles* represent same estimates at given SiO_2 contents in the rocks. The *solid modeled line* corresponds to fractional crystallization of an average iron-enriched basaltic andesite, calculated at *NNO* + 0.5 using new version of COMAGMAT-3.5. **C** Same results in FeO - log f_{O_2} coordinates. **D** Same results in FeO - SiO_2 coordinates. The *dashed line* corresponds to equilibrium crystallization of an average plagioclase-rich diabase, calculated at *NNO* + 0.5 in the range of 0–30% crystallized

technique, based on the use of the COMAGMAT-3.5 model. If we assume that the leucocratic, largely aphyric rocks represent liquids generated by fractionation, these melts should be simultaneously saturated with silicates (plagioclase + clinopyroxene) and Fe-Ti oxides (magnetite). In that case, the temperature of saturation for each rock (melt) can be calculated from plagioclase-melt or pyroxene-melt geothermometers. For this purpose we used the plagioclase thermometers of COMAGMAT, which exhibit an accuracy of 10–15 °C (Ariskin et al. 1993). Temperatures calculated for each leucocratic rock cover the range from 1125 °C for iron-enriched gabbrodiorites to 1050 °C for granophyres (Fig. 11B).

To estimate the redox conditions corresponding to *Pl-Mt* saturation, a series of calculations at different log f_{O_2} ranging from −10 to −7 were carried out for all of the leucocratic rocks, using the "magnetite" model described in the paper. A single value for log f_{O_2} for each rock was defined, at which the magnetite calculated temperature differs from that of plagioclase by no more than 1 °C. These data show a small decrease of the oxygen fugacity from 10^{-8} to 10^{-9} bar with decreasing plagioclase-magnetite temperatures (Fig. 11A). This trend corresponds approximately to *NNO* + 0.5 conditions. The accuracy of this estimate is directly related to the dependence of magnetite-liquidus on oxygen fugacity, described above. If we assume mean values of 15–30 °C/log f_{O_2}, an error of 15 °C for magnetite temperature represents the error from 1 to 0.5 log units for the estimated log f_{O_2} value.

An independent test of the f_{O_2} estimates is to simulate the crystallization of a basaltic andesite parent at *NNO* + 0.5 (Fig. 11). A typical ferrogabbro-diorite composition was used here as a parental melt (Table 3). The calculated liquid line of descent (Fig. 11D) reproduces the observed FeO-SiO_2 relations within model error. Note that another line calculated for the equilibrium crystallization of an average Chazhma plagiodolerite (Table 3) came to the point of silica depleted and iron enriched compositions similar to those of Kronotsky ferrobasalts (Barmina et al. 1989).

Conclusions

We have presented a system of empirically calibrated magnetite-melt and ilmenite-melt equilibrium equations which allow us to develop models for calculating *Mt* and *Ilm* crystallization temperatures. These expressions are calibrated for mafic melts using five component magnetites (Fe^{3+}, Fe^{2+}, Ti^{4+}, Mg^{2+}, and Al^{3+}), and exhibit accuracy of 0.5–2 mol% and 10–15 °C. They have been integrated into the COMAGMAT-3.5 program, which can be now successfully applied to a wide range of magma compositions to study the effects of temperature and oxygen fugacity on the stability and phase equilibria of Fe-Ti oxides.

On the basis of the updated COMAGMAT-3.5 phase equilibria model a new technique was proposed aimed at the estimating the redox conditions of the crystallization of magnetite-bearing mineral assemblages. Application of this approach to the tholeiitic series of Chazhma sill indicates that the oxygen fugacity was similar to $NNO + 0.5$. Numerical simulation of fractional crystallization of an iron-enriched basaltic andesite parent at these oxidizing conditions accurately reproduced the FeO-SiO_2 relations observed in the Chazhma suite.

Acknowledgments This research was supported by grants from Russian Foundation of Basic Research (96-05-64231 and 96-07-89054). We are grateful to Roger Nielsen (Oregon State University) for reading an earlier version of the manuscript and its translation, and for providing comments which materially improved the manuscript. We thank D. Snyder and an anonymous reviewer for thorough and thoughtful reviews.

References

Ariskin AA (1998) Calculation of titanomagnetite stability on the liquidus of basalts and andesites with special reference to tholeiitic magma differentiation. Geochem Int 36: 18–27

Ariskin AA, Nikolaev GS (1996) An empirical model for the calculation of spinel-melt equilibria in mafic igneous systems at atmospheric pressure: 1. chromian spinels. Contrib Mineral Petrol 123: 282–292

Ariskin AA, Barmina GS, Frenkel MYa (1987) Computer simulation of basalt magma crystallization at a fixed oxygen fugacity. Geochem Int 24: 92–100

Ariskin AA, Frenkel MYa, Barmina GS, Nielsen RL (1993) COMAGMAT: a Fortran program to model magma differentiation processes. Computers and Geosciences 19: 1155–1170

Ariskin AA, Barmina GS, Meshalkin SS, Nikolaev GS, Almeev RR (1996) INFOREX-3.0: a database on experimental studies of phase equilibria in igneous rocks and synthetic systems. II. Data description and petrological applications. Computers and Geosciences 22: 1073–1082

Ariskin AA, Meshalkin SS, Almeev RR, Barmina GS, Nikolaev GS (1997) INFOREX information retrieval system: analysis and processing of experimental data on phase equilibria in igneous rocks. Petrology 5: 28–36

Auwera JV, Longhi J (1994) Experimental study of a jotunite (hypersthene monzodiorite): constraints on the parent magma composition and crystallization conditions (P, T, f_{O_2}) of the Bjerkreim-Sokndal layered intrusion (Norway). Contrib Mineral Petrol 118: 60–78

Barmina GS, Ariskin AA, Frenkel MYa, Kononkova NN (1988) Origin of the Chazhma-sill ferrodiorites. Geochem Int 25: 110–114

Barmina GS, Ariskin AA, Frenkel MYa (1989) Petrochemical types and crystallization conditions of the Kronotsky Peninsula plagiodolerite (Eastern Kamchatka). Geochem Int 26: 24–37

Barmina GS, Ariskin AA, Kolesov GM (1992) Simulating the REE spectra of hypabyssal rocks in the Kronotsky series, Eastern Kamchatka. Geochem Int 29: 45–54

Bolikhovskaya SV, Vasil'yeva MO, Koptev-Dvornikov EV (1996) Simulating low-Ca pyroxene crystallization in basite systems: new geothermometer versions. Geochem Int 33: 1–19

Borisov AA, Shapkin AI (1990) A new empirical equation relating Fe^{3+}/Fe^{2+} in magmas to their composition, oxygen fugacity, and temperature. Geochem Int 27: 111–116

Brooks CK, Larsen LM, Nielsen TFD (1991) Importance of iron-rich tholeiitic magmas at divergent plate margins: a reappraisal. Geology 19: 269–272

Camur MZ, Kilinc AI (1995) Empirical solution model for alkalic to tholeiitic basic magmas. J Petrol 36: 497–514

Chalokwu CI, Grant NK, Ariskin AA, Barmina GS (1993) Simulation of primary phase relations and mineral compositions in the Partridge River intrusion, Duluth Complex, Minnesota: implications for the parent magma composition. Contrib Mineral Petrol 114: 539–549

Eggler DH, Osborn EF (1982) Experimental studies of the system MgO-FeO-Fe_2O_3-$NaAlSi_3O_8$-$CaAl_2Si_2O_8$-SiO_2 – a model for subalkaline magmas. Am J Sci 282: 1012–1041

Frenkel MYa, Ariskin AA (1984) A computer algorithm for equilibration in a crystallizing basalt magma. Geochem Int 21: 63–73

Frenkel MYa, Yaroshevsky AA, Ariskin AA, Barmina GS, Koptev-Dvornikov EV, Kireev BS (1989) Convective-cumulative model simulating the formation process of stratified intrusions. In: Bonin B, Didier J, Le Fort P, Propach G, Puga E, Vistelius AB (eds) Magma-crust interactions and evolution. Theophrastus Publications SA, Athens-Greece, pp 3–88

Fudali RF (1965) Oxygen fugacities of basaltic and andesitic magmas. Geochim Cosmochim Acta 29: 1063–1075

Ghiorso MS (1985) Chemical mass transfer in magmatic processes I. Thermodynamic relations and numeric algorithms. Contrib Mineral Petrol 90: 107–120

Ghiorso MS, Carmichael ISE (1985) Chemical mass transfer in magmatic processes II. Applications in equilibrium crystallization, fractionation and assimilation. Contrib Mineral Petrol 90: 121–141

Ghiorso MS, Sack RO (1995) Chemical mass transfer in magmatic processes IV. A revised and internally consistent thermodynamic model for the interpolation and extrapolation of liquid-solid equilibria in magmatic systems at elevated temperatures and pressures. Contrib Mineral Petrol 119: 197–212

Grove TL, Baker MB (1984) Phase equilibrium controls on the tholeiitic versus calc-alkaline differentiation trends. J Geophys Res 89B: 3253–3274

Grove TL, Juster TC (1989) Experimental investigations of low-Ca pyroxene stability and olivine-pyroxene-liquid equilibria at 1-atm in natural basaltic and andesitic liquids. Contrib Mineral Petrol 103: 287–305

Grove TL, Kinzler RJ (1986) Petrogenesis of andesites. Ann Rev Earth Planet Sci 14: 417–454

Hill R, Roeder P (1974) The crystallization of spinel from basaltic liquid as a function of oxygen fugacity. J Geol 82: 709–729

Hunter RH, Sparks RSJ (1987) The differentiation of the Skaergaard intrusion. Contrib Mineral Petrol 95: 451–461

Juster TC, Grove TL (1989) Experimental constraints on the generation of the FeTi basalts, andesites, and rhyodacites at the Galapagos Spreading Center, 85 W and 95 W. J Geophys Res 94B: 9251–9274

Kilinc A, Carmichael ISE, Rivers ML, Sack RO (1983) The ferric-ferrous ratio of natural silicate liquids equilibrated in air. Contrib Mineral Petrol 83: 136–140

Kress VC, Carmichael ISE (1988) Stoichiometry of the iron oxidation reaction in silicate melt. Am Mineral 73: 1267–1274

Kress VC, Carmichael ISE (1991) The compressibility of silicate liquids containing Fe_2O_3 and the effect of composition, temperature, oxygen fugacity and pressure on their redox states. Contrib Mineral Petrol 108: 82–92

Longhi J (1991) Comparative liquidus equilibria of hypersthene-normative basalts at low pressure. Am Mineral 76: 785–800

Meshalkin SS, Ariskin AA (1996) INFOREX-3.0: a database on experimental studies of phase equilibria in igneous rocks and synthetic systems. I. Datafile and management system structure. Computers and Geosciences 22: 1061–1071

Mysen BO (1991) Relations between structure, redox equilibria of iron, and properties of magmatic liquids. In: Perchuk LL, Kushiro I (eds) Physical chemistry of magmas. (Advances in Physical Geochemistry vol. 9). Springer-Verlag, New York, pp 41–98

Mysen BO, Virgo D, Neumann E-R, Seifert FA (1985) Redox equilibria and the structural states of ferric and ferrous iron in melts in the system CaO-MgO-Al_2O_3-SiO_2-Fe-O: relationships between redox equilibria, melt structure and liquidus phase equilibria. Am Mineral 70: 317–331

Nielsen RL (1990) Simulation of igneous differentiation processes. In: Nicholls J, Russell JK (eds) Modern methods of igneous petrology: understanding magmatic processes. (Reviews in Mineralogy vol. 24). Mineralogical Society of America, Washington DC, pp 63–105

Nielsen RL, Dungan MA (1983) Low-pressure mineral-melt equilibria in natural anhydrous mafic systems. Contrib Mineral Petrol 84: 310–26

Nielsen RL, Forsythe LM, Gallahan WE, Fisk MR (1994) Major- and trace-element magnetite-melt equilibria. Chem Geol 117: 167–191

Nikolaev GS, Borisov AA, Ariskin AA (1996) Calculation of the ferric-ferrous ratio in magmatic melts: testing and additional calibration of empirical equations for various magmatic series. Geochem Int 34: 641–649

Osborn EF (1959) Role of oxygen pressure in the crystallization and differentiation of basaltic magma. Am J Sci 257: 609–647

Presnall DC (1966) The join forsterite-diopside-iron oxide and its bearing on the crystallization of basaltic and ultramafic magmas. Am J Sci 264: 753–809

Sack RO, Ghiorso MS (1991) An internally consistent model for the thermodynamic properties of Fe-Mg-titanomagnetite-aluminate spinels. Contrib Mineral Petrol 106: 474–505

Sack RO, Carmichael ISE, Rivers M, Ghiorso MS (1980) Ferric-ferrous equilibria in natural silicate liquids at 1 bar. Contrib Mineral Petrol 75: 369–376

Shi P (1993) Low-pressure phase relationships in the system Na_2O-CaO-FeO-MgO-Al_2O_3-SiO_2 at 1100 °C, with implications for the differentiation of basaltic magmas. J Petrol 34: 743–762

Shibata K (1967) The oxygen partial pressure of the magma from Mihara volcano, O-sima, Japan. Bull Chem Soc Japan 40: 830–834

Sisson TW, Grove TL (1993) Experimental investigations of the role of H_2O in calc-alkaline differentiation and subduction zone magmatism. Contrib Mineral Petrol 113: 143–166

Snyder D, Carmichael ISE, Wiebe RA (1993) Experimental study of liquid evolution in a Fe-rich, layered mafic intrusion: constraints of the Fe-Ti oxide precipitation on the T-f_{O_2} and T-ρ paths of tholeiitic magmas. Contrib Mineral Petrol 113: 73–86

Stormer JC Jr (1983) The effects of recalculation on estimates of temperature and oxygen fugacity from analyses of multicomponent iron-titanium oxides. Am Mineral 68: 586–594

Thornber CR, Roeder PL, Foster JR (1980) The effect of composition on the ferric-ferrous ratio in basaltic liquids at atmospheric pressure. Geochim Cosmochim Acta 44: 525–532

Thy P, Lofgren GE (1994) Experimental constraints on the low-pressure evolution of transitional and mildly alkalic basalts: the effect of Fe-Ti oxide minerals and the origin of basaltic andesites. Contrib Mineral Petrol 116: 340–351

Toplis MJ, Carroll MR (1995) An experimental study of the influence of oxygen fugacity on Fe-Ti oxide stability, phase relations, and mineral-melt equilibria in ferro-basaltic systems. J Petrol 36: 1137–1170

Toplis MJ, Carroll MR (1996) Differentiation of ferro-basaltic magmas under conditions open and closed to oxygen: implications for Skaergaard intrusion and other natural systems. J Petrol 37: 837–858

Toplis MJ, Libourel G, Carroll MR (1994) The role of phosphorus in crystallization processes of basalt: an experimental study. Geochim Cosmochim Acta 58: 797–810

Weaver JS, Langmuir CH (1990) Calculation of phase equilibrium in mineral-melt systems. Computers and Geosciences 16: 1–19

Yang H-J, Kinzler RJ, Grove TL (1996) Experiments and models of anhydrous, basaltic olivine-plagioclase-augite saturated melts from 0.001 to 10 kbar. Contrib Mineral Petrol 124: 1–18